

COVER SHEET
for
The Fourteenth International Conference on Vacuum Web Coating

Title of Paper: “Thermal Evaporation of Li: Experiment and a Novel Thermodynamic Model”

Names of Authors: John Affinito, Mike McCann, and Chris Sheehan

Full Name of Principal Author to Receive All Correspondence: John David Affinito

Full Mailing Address of Principal Author: John Affinito, Ph.D.
Senior Director of Vacuum Technology
Moltech Corporation
9062 South Rita Road
Tucson, Arizona
U.S.A., 85747-9018
(520) 799-7509 (phone)
(520) 799-7501 (fax)
John.Affinito@Moltech.com (e-mail)
MrPML@Hotmail.com (e-mail)

Telephone Number: (520) 799 - 7509 (phone)

Telefax Number: (520) 799 - 7501 (fax)

“Thermal Evaporation of Li: Experiment and a Novel Thermodynamic Model”

John Affinito*, Michael J. McCann† and Chris Sheehan*

***Moltech Corporation
9062 South Rita Road
Tucson, Arizona, 85747
520 – 799 – 7500 (phone)
520 – 799 – 7501 (fax)**

John.Affinito@Moltech.com

**†McCann Science
PO Box 902
Chadds Ford, PA, 19317
302 - 654 - 2953 (phone)
302 - 429 - 9458 (fax)**

mjmccann@iee.org

ABSTRACT: Lithium metal has been thermally evaporated onto Polyethylene Teraphthalate (PET) substrate, from a large open reservoir whose top is approximately 1 cm from the substrate, in a roll-to-roll vacuum web coating process. A self-consistent thermodynamic model is developed and used to calculate the Li flux to the substrate with no free parameters. The model calculates an effective temperature for the Li gas based upon a mass balance relationship. The number of atoms emitted from the molten Li surface plus those emitted from the crucible walls is set equal to the number of atoms adhering to the substrate plus those atoms lost to the surroundings through the reservoir-substrate edge gaps plus those atoms impinging onto the crucible walls. Those atoms lost to the surroundings, or interacting with cooler surfaces and returning to the gas, effectively cool the Li gas. The effective Li gas temperature is then calculated from the mass balance equations and used to calculate a Li impingement rate onto the substrate. Input to the model is the measured Li liquid and reservoir wall temperatures and the measured areas of the exposed substrate and reservoir-substrate gaps. The model predictions for the Li film thickness are compared to measurements and are found to agree within the instrumentation errors inherent in the measuring device ($\pm 5\%$). The substrate heat load, due to the deposition process, has also been modeled in order to optimize the Li deposition rate while minimizing substrate damage. Substrate heating due to both radiation and Li condensation are accounted for. The temperature rise of the substrate is calculated based upon the Li flux, reservoir temperature and geometry and the cooling drum temperature. Free parameters in this last step are the emissivity of the Li/PET surface and the heat transfer coefficient between the PET and the drum. The model predictions for substrate heating, which also appear very reasonable, will be discussed briefly here and in more detail in a future publication once in situ substrate temperature measurements are available for comparison with the model calculations.

INTRODUCTION: Vapor deposited Li metal, on flexible polymer substrates, is of interest for use as anode material in a variety of batteries for commercial electronics, power tools or electric vehicles. However, the thickness of Li required is generally in excess of 10 μm , with the precise thickness depending upon the specific operational requirements of the desired battery. To deposit such a thick Li film, at line speeds that would be commercially attractive, places a severe heat load on the polymer substrate. For a variety of practical reasons, the substrate of choice is presently Polyethylene Terephthalate, or PET. PET has a glass transition temperature of $T_g=70\text{ C}^1$. Thus, in principle, when coating PET, the PET substrate can distort and undergo irreversible damage at temperatures as low as T_g . However, PET is found to retain its mechanical properties to as high as 120 C in some instances¹. The exact damage threshold can depend upon substrate gauge, tensioning, the length of time that the substrate is at temperature and, relative to the particular process/product, the definition of what actually constitutes damage. When depositing Li, if the film PET substrate distorts to the point where a wrinkle occurs, and any part of the substrate lifts from the cooling drum, the film burns through. It is therefore crucial to process the film under heat load conditions that do not exceed this point.

A first step in modeling the substrate heat load, in order to optimize the deposition rate and minimize the heat load to the substrate, is to understand the Li flux and thermal radiation emissions from the Li source. At Moltech, in collaboration with McCann Sciences, we have developed a detailed, proprietary, numerical modeling tool (which is still evolving) to determine the heat load to a web substrate in a general vacuum deposition process. The numerical implementation of this model is within the Mathcad 2000 software environment. The implementation is of a modular nature that permits multiple sources of various types to be arrayed randomly along the web path. The focus of this work will be thermal sources only.

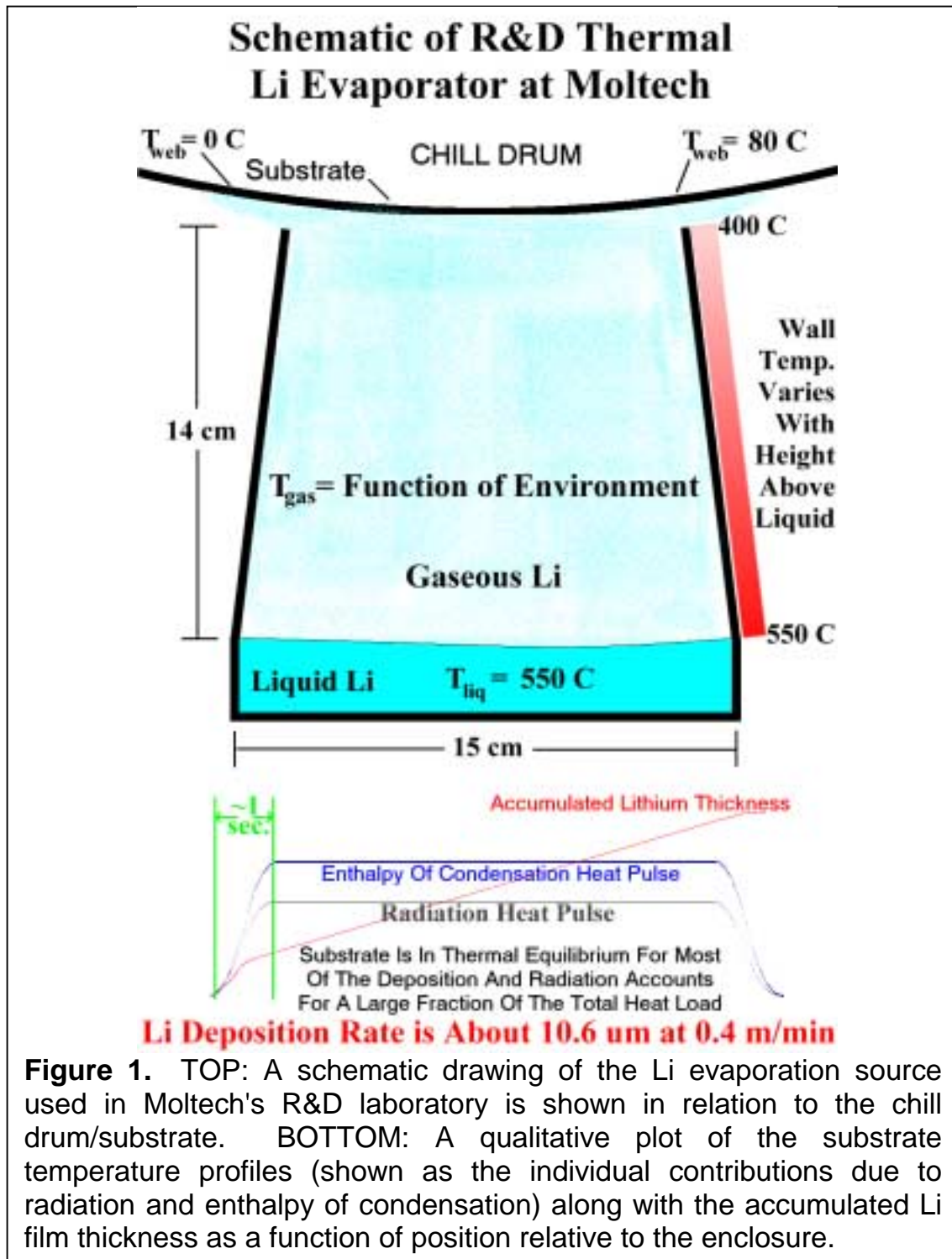
Our numerical model predictions agree extremely well with those system parameters that we can, at present, measure. As well, the model predictions appear to be quite reasonable, and qualitatively correct, for those parameters that we can estimate but cannot yet measure. In this work we will develop a general thermodynamic model for the calculation of evaporated flux from a thermal crucible that is central to the problem of modeling the heat load to the substrate during Li deposition. We then tailor the general model to the specific geometry of the Li evaporation source used in the R&D laboratory at Moltech. Since we can measure the thickness of the deposited Li film, we can easily compare the predictions to the actual experimental results.

A brief discussion of the radiation emission, substrate heat load and substrate-to-drum heat transfer coefficient will be given and the substrate heating model predictions will be discussed. However, we have not yet implemented an in situ method to measure the substrate temperature as it travels through the deposition zone. In a future publication we will go into more detail on these portions of the model and, at that time, we intend to make direct comparisons of the calculated substrate temperature profile as a function of position relative to the Li source and the measured substrate temperature profile. At this time we will discuss the details of our Li evaporation source and our Li deposition experiments².

EXPERIMENTAL DETAILS: An artist's rendition/schematic drawing of our Li source and substrate are shown in the top half of Figure 1. The Li evaporation crucible consists of two main regions. First is a bottom portion that is a cartridge heated square pan, 15 cm on edge by 2 cm deep, filled with molten Li. Second, rising from the square Li pan, the walls gradually taper to form a square aperture, 14 cm on edge, 14 cm above the liquid Li. The pan and square pyramidal enclosure are welded together so that the volume between the pan and walls is completely enclosed with the exception of the square aperture at the top.

The following parameters apply to the "standard" experimental run that we will discuss in the remainder of this work. The distance between the substrate/chill drum and the crucible aperture is adjustable and, for purposes of these experiments, is maintained at 1 cm. The web is 93 gauge PET (23 μm) and the web speed is 0.4 m/min (2/3 cm/s). Before power is applied to the cartridge heaters in the base of the Li crucible/enclosure, the vacuum chamber is evacuated to 2×10^{-6} torr, or lower. Once heater power is applied it takes about 20 minutes for the Li to melt and for the liquid to stabilize at $T_{\text{liq}}=550$ C. When the liquid first reaches 550 C the temperature at the top of the enclosure is only about $T_{\text{wall}}^{\text{Top}}=360$ C. After 20 additional minutes $T_{\text{wall}}^{\text{Top}}$ stabilizes at about $T_{\text{wall}}^{\text{Top}}=400$ C.

Deposition is predicted to, and certainly should, be fairly constant directly above the enclosure and taper to near zero by about 1 cm outside of the enclosure. The bottom of Figure 1 shows, qualitatively, the model predictions for the substrate temperature profiles (shown as the individual contributions due to radiation and enthalpy of condensation) along with the accumulated Li film thickness as a function of position relative to the enclosure. After a deposition run the Li thickness is measured with a piston micrometer (Starrett F2720-0) that is



accurate to $\pm 0.5 \mu\text{m}$. The thermodynamic model for calculating evaporated flux levels will be developed next.

DEVELOPMENT OF A GENERAL EVAPORATED FLUX MODEL AND COMPARISON OF OUR SYSTEM TO THE MODEL:

When, at the surface of a liquid, the kind and number of atoms, or molecules, entering the gas phase from the liquid surface is equal to the kind and number of atoms, or molecules, that enter the liquid from the gas phase at that same surface it is said that the liquid is in equilibrium with its vapor. The relationship between the equilibrium vapor pressure, liquid evaporation rate at the surface and the temperatures of the liquid and gas has been studied for a large number of materials and most elements. The mathematical expression that relates the equilibrium mass evaporation rate to the liquid, or gas, temperature has a common functional form for most elemental liquids. This general mathematical expression is derived from the thermodynamic expressions for the enthalpy and free energy of the material. The expression contains both material parameters (like molecular weight) for the particular element of interests along with some arbitrary constants and the liquid or gas temperature. The arbitrary constants are fitted through experimental measurements of temperature and vapor pressure. Chapter 10 of Scientific Foundations of Vacuum Technique, by S. Dushman and J.M. Lafferty³ contains one such functional form for this expression for elemental liquids in equilibrium with their vapor along with a compilation of the fitted constants for most of the elements. Equation 1 is this functional relation for elemental Li where all of the material parameters and fitted constants have been combined and reduced to numbers to leave a functional form that appears to vary only with the temperature of the liquid, or gas. Thus, for liquid Li in equilibrium with its vapor³

$$W(T_{liq}) = 10^{\left[7.18 - 0.5 \text{LOG}(T_{liq}) - \frac{8070}{T_{liq}}\right]}, \quad \frac{g}{cm^2 s}, \quad \text{Equation 1}$$

where, with liquid and vapor in thermal equilibrium at temperature $T_{liq}=T_{gas}$, W is the mass flux of Li atoms leaving from (or returning to) the liquid Li surface per second per square centimeter of liquid Li surface. In Equation 1 W depends only on T_{liq} , which is assumed equal to T_{gas} due to the condition of equilibrium. In Equation 1, as in all other equations to follow, all temperatures should be *inserted* in degrees Kelvin, even though temperatures will be reported in degrees Celsius, or C, throughout the text. In all other cases cgs units are to be *inserted* into the equations even though some quantities may be reported in other units and, in Equation 5, the film thickness value is actually calculated in microns (μm) from *inserted* cgs units.

To these authors there did not appear to be any reason to assume that Equation 1 would not describe the rate at which atoms are either emitted from *any* surface to, or impinge upon *any* surface from, the gas phase. We assume this to be true under non-equilibrium conditions as well as under equilibrium conditions for the work that will now be described.

In other words, we postulate the following. When a liquid source is present somewhere in the system, Equation 1 will predict the emission and absorption rates at all surfaces in the system. This is regardless of whether the liquid and gas temperatures are equal or not ($T_{\text{liq}}=T_{\text{surface}}=T_{\text{gas}}$ and $T_{\text{liq}}\neq T_{\text{surface}}\neq T_{\text{gas}}$) and whether or not the *net* flux across the liquid-gas interface is zero or non-zero.

We assume the above postulate to be true even when the impingement from, or emission to, the gas phase is at a surface that is not the liquid reservoir that is the original source of all of the gaseous and liquid material under discussion.

Such non-equilibrium conditions obviously exist in all thermal evaporation deposition processes since, by virtue of the very act of deposition, some species that leave the liquid can never return. As well, many of the gas phase species impinge on surfaces other than the liquid or substrate. In the latter situations it is observed that, over time, a net increase, or decrease, in these species adhered to that surface can be observed. It is usual to speak of the sticking coefficient of the species relative to the surface and to say that, upon impingement, sometimes they stick and sometimes they do not stick or that they bounce off or are re-emitted from the surface to the gas phase. In our model we assume that, when only thermal processes are considered, all impinging atoms or molecules stick to the surface and that, independently of this impingement/sticking, other atoms and molecules are emitted from the surface. The modeled impingement and emission rates can then be calculated from Equation 1 where the gas and surface temperatures are not necessarily equal. Further, the loss of the permanently deposited species, and the impingement and emission interactions of other species with various surfaces, must alter the gas temperature. For deposition, and for interactions with surfaces cooler than the liquid, the effect of these processes must be to reduce the temperature of the gas relative to the temperature of the liquid (i.e. $T_{\text{gas}} < T_{\text{liq}}$).

Thus, this model permits calculation of both deposition rates on a substrate, from an open source under non-equilibrium conditions, and the sticking coefficients for any surfaces in the system provided the liquid, gas and surface temperatures are known. One assumes that all species hitting the surface, as predicted by

Equation 1, stick. However, independently, species are constantly emitted from the surface according to Equation 1. The sticking coefficient (k_s) at a surface is then simply given as

$$k_s = 1 - \frac{\text{emission rate}}{\text{impingement rate}} = 1 - \frac{W(T_{wall})}{W(T_{gas})}, \quad \text{Equation 2}$$

where the impingement and emission rates are calculated from Equation 1. With this model, because of the power law dependence of the mass flux in Equation 1, it is obvious why metals condense with virtually unity sticking coefficient on ambient temperature substrates. Similarly the model tells us something else that we already know to be true. That is that most any vapor has, for practical purposes, a sticking coefficient of 1 on any surface cooled below the melting point of the vapor's solid phase. Of course chemical reactions, or physical bombardment, would modify the emission, or impingement, coefficients since these are not thermal processes as defined above in Equations 1 and 2. Now we will investigate how the model handles the R&D Li evaporator in our laboratory - a situation where we did not know the answer ahead of time.

To determine the deposition rate from our thermal evaporation crucible it is necessary to perform a mass balance by counting all of the atoms that move between the gas phase and all of the surfaces in the system. Details of this procedure will now be developed.

Using Equation 1, we find that the flux (F_0) leaving the surface of the liquid Li in the reservoir is given as

$$F_0 = W(T_{liq}) A_{liq}, \quad \frac{g}{s}, \quad \text{Equation 3.0}$$

where A_{liq} is the area of the liquid surface (about 15 cm X 15 cm for our crucible). Similarly, the flux (F_1) returning to the surface of the liquid Li in the reservoir is given as

$$F_1 = W(T_{gas}) A_{liq}, \quad \frac{g}{s}, \quad \text{Equation 3.1}$$

where T_{gas} is the temperature of the gaseous Li vapor within the crucible/substrate volume. Likewise, the flux (F_2) escaping through the gap between the top of the crucible and the substrate is given as

$$F_2 = W(T_{gas}) A_{GAP}, \quad \frac{g}{s}, \quad \text{Equation 3.2}$$

where A_{GAP} is the area of the gap (about 4 X 1 cm X 14 cm for our crucible).

The flux striking, and depositing onto, the substrate (F_3) is given as

$$F_3 = W(T_{gas}) A_{web}, \quad \frac{g}{s}, \quad \text{Equation 3.3}$$

where A_{web} is the area of the web exposed to Li flux, which is approximately the area of the open aperture at the top of the crucible (about 14 cm X 14 cm in our crucible). Note that we will assume that emission processes are negligible at the substrate. That is, we are assuming a substrate sticking coefficient of 1 according to Equation 2. If we were to include the emission equation, $F_{WebEmission} = W(T_{web}) A_{web}$, we would have found an insignificant emitted flux due to the low web temperature (~ 0 C), relative to the melting point of Li (182 C) coupled with the power law behavior of Equation 1.

The flux that is emitted from the crucible walls (F_4), assuming isothermal conditions across the surface of the walls, is given as

$$F_4 = W(T_{wall}) A_{wall}, \quad \frac{g}{s}, \quad \text{Equation 3.4}$$

where T_{wall} is the temperature of the crucible wall and A_{wall} is the area of the crucible wall (about 4 X 14.5 cm X 14 cm for our crucible).

Lastly, the flux (F_5) that impinges, and condenses, on the crucible walls is given as

$$F_5 = W(T_{gas}) A_{wall}, \quad \frac{g}{s}. \quad \text{Equation 3.5}$$

Remember that, under our model: condensation onto the walls (F_5) depends only on the gas temperature (T_{gas}), and not the wall temperature (T_{wall}); emission from the wall (F_4) depends only on the wall temperature (T_{wall}), and not the gas temperature (T_{gas}); and impingement and emission processes are independent of each other.

For our crucible, we know from measurements that the assumption of an isothermal wall in Equation 3.4 is false. The temperature of the walls of our crucible is not constant over the entire interior surface. In our “standard” run, we have measured the wall temperature and it varies from 550 C at the surface of the liquid to only 400 C at the top edge near the substrate. Therefore, Equation 3.4 is likely to be a poor approximation to F_4 since, by Equation 1, the flux leaving a surface should have a power law dependence on the temperature of that surface and the wall supports a very large temperature gradient. Thus, F_4 would more

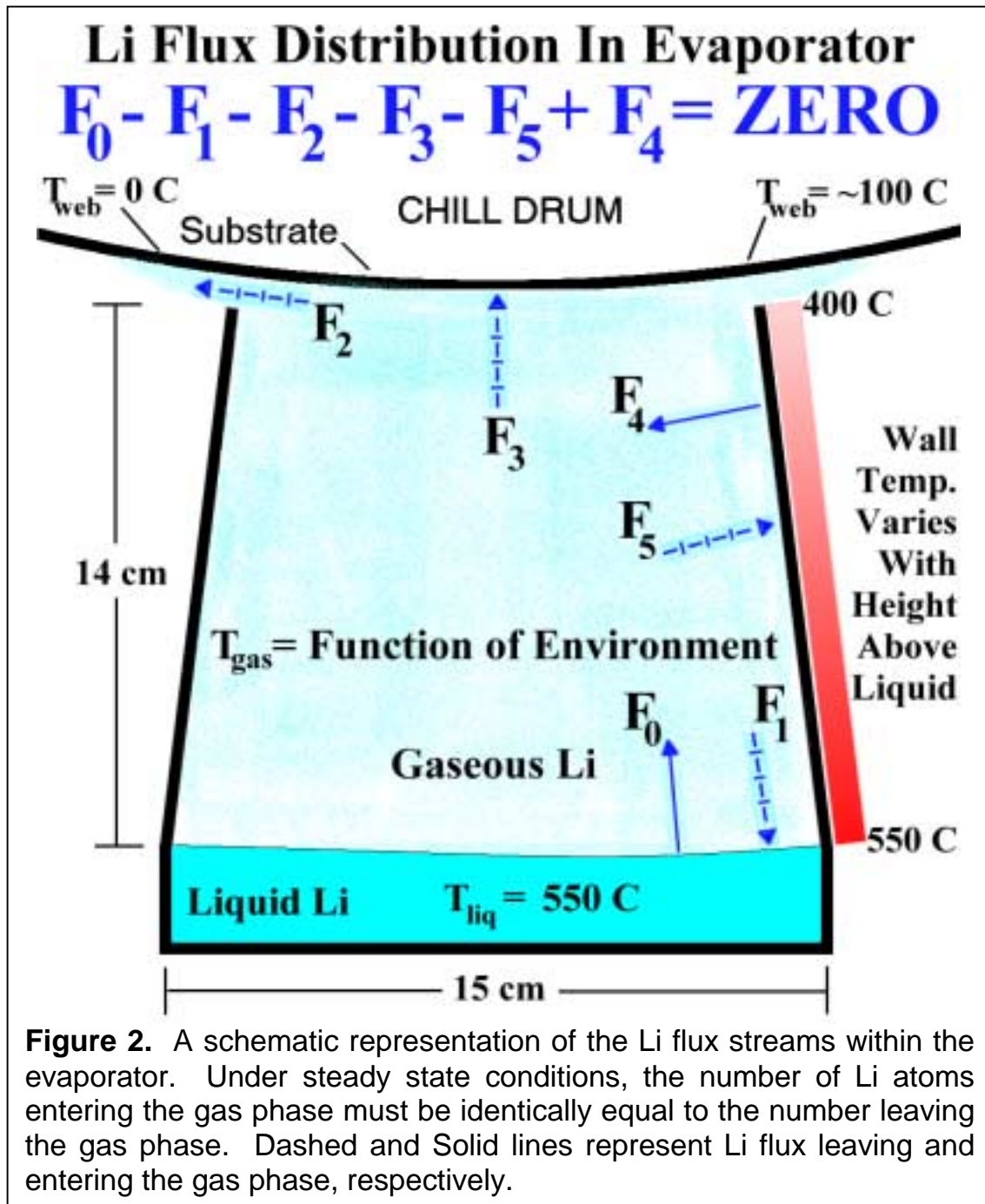


Figure 2. A schematic representation of the Li flux streams within the evaporator. Under steady state conditions, the number of Li atoms entering the gas phase must be identically equal to the number leaving the gas phase. Dashed and Solid lines represent Li flux leaving and entering the gas phase, respectively.

accurately reflect reality if the positional dependence of T_{wall} , over the surface A_{wall} , were incorporated into the calculation.

Recall that the bottom portion of our Li evaporation crucible consists of a cartridge heated square pan, 15 cm on edge, filled with molten Li. Rising from

the square Li pan, the walls gradually taper to form a square aperture, 14 cm on edge, 14 cm above the liquid Li. For purposes of calculating the flux (F_4) emitted from the interior surface walls of the crucible (A_{wall}) we can view the 4 sides of our square pyramidal enclosure as 4 trapezoids. These trapezoids have edge length $L_B=15$ cm at the bottom, and edge length $L_T=14$ cm at the top with $\Delta L=L_B-L_T$. Since the pyramid is square, with height $H'=14$ cm, we find H , the height of each of the 4 tilted trapezoidal walls, to be

$$H = \frac{H'}{\cos\left(\tan^{-1}\left(\frac{\Delta L}{2H'}\right)\right)} \text{ cm.}$$

Symmetry considerations dictate that the temperature variation over the wall will be, primarily, in the perpendicular direction along the wall from the bottom towards the top. A linear temperature gradient in this direction is then a reasonable starting approximation. Taking h as the coordinate in the perpendicular direction from the base, along the surface of the wall, toward the top of the trapezoid, we write $L(h)$ as the width of each trapezoid at perpendicular distance h measured along the wall from the base toward the top of the wall. In general then, we can rewrite Equation 1 with T_{wall} as a function of h . We then substitute the new Equation 1 into Equation 3.4 and integrate over the 4 trapezoidal walls using the wall coordinate h as the variable of integration. This gives F_4 as

$$F_4 = 4 \int_0^H W(T_{wall}(h))L(h)dh, \quad \frac{g}{s} \quad \text{Equation 3.4.1}$$

where F_4 now takes into account the fact that the wall temperature varies with position and that the flux emission varies locally with the temperature variations.

Finally, explicitly including the linear gradient-in- h dependencies of the wall temperature and trapezoidal wall widths, specific to our evaporator, into the expressions for W and L in Equation 3.4.1 we find F_4 to be

$$F_4 = 4 \int_0^H W\left(\left[T_{liq} - \frac{\Delta T_{wall}}{H} h\right]\right) \left[L_B - \frac{\Delta L}{H} h\right] dh, \quad \frac{g}{s},$$

Equation 3.4.2

where the temperature is now assumed to vary linearly from the liquid temperature (T_{liq}) at the bottom of the wall to the measured temperature (T_{wall}^{Top}) at the top of the wall and $\Delta T_{wall}=T_{liq}-T_{wall}^{Top}$ is the temperature difference between the bottom and the top of the wall.

Under steady state conditions, in order to maintain mass and energy balance, the total number of atoms must be conserved. This means that, in steady state, at any instant the total number of Li atoms entering the gas phase from the liquid surface plus those emitted from the walls, must exactly equal the total number leaving the gas phase through impingement on the walls and substrates plus those escaping through the gaps plus those returning to the liquid surface. Therefore, the identity of Equations 4, below, must hold true under steady state conditions.

$$F_0 - F_1 - F_2 - F_3 - F_5 + F_4 = ZERO, \quad \text{Equation 4.1}$$

or

$$\begin{aligned} & W(T_{liq}) A_{liq} - W(T_{gas}) A_{liq} - W(T_{gas}) A_{GAP} \\ & - W(T_{gas}) A_{web} - W(T_{gas}) A_{wall} \\ & + 4 \int_0^H W \left(\left[T_{liq} - \frac{\Delta T_{wall}}{H} h \right] \right) \left[L_B - \frac{\Delta L}{H} h \right] dh = ZERO, \end{aligned}$$

$$\text{Equation 4.2}$$

Figure 2 depicts the flux distribution identity of Equations 4 in a schematic fashion. In Equation 4.2, all quantities with the exception of T_{gas} are known. Thus, Equation 4.2 can be solved for the volume distribution of T_{gas} values that make the identity true. We will assume that T_{gas} is constant over the entire volume. The isothermal assumption will then be justified by the predictions. A physical plausibility argument, as to why we might expect the gas volume to be isothermal, will also be presented. Once T_{gas} is known, the thickness that accumulates on the substrate can be calculated from $W(T_{gas})$, the known density of Li metal and the period of time (Δt) during which the substrate is exposed to the gaseous flux. For our web system, Δt is given as the length of the deposition aperture ($L_T=14$ cm for our crucible) divided by the web speed (.4 m/min, or 2/3 cm/s, in our standard run). This gives $\Delta t=21$ seconds for our crucible and our standard run. In general, the thickness (d) of the Li film, in microns, can be calculated as

$$d = W(T_{gas}) \frac{\Delta t}{\rho_{Li}} 10^4, \quad \mu m, \quad \text{Equation 5}$$

where ρ_{Li} is 0.534 g/cm³.

In our standard run, where $T_{liq}=550$ C, *measurements* show that T_{wall}^{Top} comes to equilibrium as much as 20 minutes after the time when T_{liq} is stable. The

measured thickness of the Li film varies from about $10 \mu\text{m} \pm 0.5 \mu\text{m}$ when T_{liq} first reaches equilibrium, and $T_{\text{wall}}^{\text{Top}}$ is about 360 C, to about $11 \mu\text{m} \pm 0.5 \mu\text{m}$ after 20 additional minutes when $T_{\text{wall}}^{\text{Top}}$ is about 400 C. If, as far as flux absorption and emission processes are concerned, the walls are neglected entirely in Equations 4.2 and 5, one calculates $T_{\text{gas}} \approx 523 \text{ C}$ with a Li thickness of about $15.3 \mu\text{m}$. Under the assumption of an isothermal wall temperature of 400 C one calculates $T_{\text{gas}} \approx 491 \text{ C}$ with a Li thickness of only about $6 \mu\text{m}$.

Using the full linear temperature gradient model, the calculation yields $T_{\text{gas}} \approx 510 \text{ C}$ with a Li thickness of $10.6 \mu\text{m}$ when $T_{\text{wall}}^{\text{Top}} = 400 \text{ C}$. Similarly, one calculates $T_{\text{gas}} \approx 506 \text{ C}$ with a Li thickness of $9.7 \mu\text{m}$ when $T_{\text{wall}}^{\text{Top}} = 360 \text{ C}$. **Within the measurement errors one sees that, with no free parameters, the full model accurately calculates the measured thickness.** Table I summarizes the model predictions for various wall temperature profiles.

The accuracy of this model calculation is even more striking when the magnitudes of the individual flux contributions (F_i , $i=0\dots5$) are examined and compared. The single largest flux element is not the flux off of the liquid surface (F_0). The flux that impinges onto the walls (F_5) is more than a third greater than F_0 . In fact the magnitude of the net flux to the walls (impingement minus emission, or $F_5 - F_4$) is nearly as large as F_0 and it *is* larger than the total of the other three flux contributions ($F_1 + F_2 + F_3$) combined. This precise mathematical balance is dependent upon two key mechanisms. One mechanism is that the gaseous Li cloud is transporting Li atoms between all of the various surfaces as if it were at the constant, and spatially uniform, temperature T_{gas} . The other key mechanism is that both absorption and emission processes, from any surface, are assumed independent and are governed by Equation 1 as postulated above and as implemented in Equations 3 and 4. The result of the latter mechanism is that, for our Li source at least, Li transport is dominated by the crucible walls. Therefore, it is crucial to understand the geometry of the crucible and the way in which that geometry affects the deposition rate and heat load to the substrate. For instance, even though the liquid Li temperature becomes stable very quickly it takes an additional 20 minutes, by both thermal conductance from the heated pan zone and interactions with the Li gas, before the temperature of the crucible walls reach their final steady state values. During those 20 minutes the deposition thickness varies by more than 10% even though the liquid temperature, and all cross-sectional areas and conductances remain constant. Thus a constant Li thickness can be maintained simply by adjusting the web speed in proportion to the measured value of $T_{\text{wall}}^{\text{Top}}$.

TABLE I

<u>Assumed Wall Temperature Profile</u>	T_{liq} (C)	T_{wall}^{Top} (C)	Calculated T_{gas} (C)	Calculated Thickness (um)	Measured Thickness (um)
<u>INERT Walls, NO GAP AND NO APERTURE</u>	550	N/A	550	32.5	9.5 - 11.5
NONE - Inert Walls neither absorb or emit	550	N/A	523	15.3	9.5 - 11.5
NONE - INERT Walls AND NO GAP	550	N/A	527	17.3	9.5 - 11.5
Isothermal at T_{wall}^{Top}	550	360	490.7	5.6	10 ± 0.5
Isothermal at T_{wall}^{Top}	550	400	491.3	5.8	11 ± 0.5
Linear Gradient from T_{liq} at bottom to T_{wall}^{Top} at top	550	360	506	<u>9.7</u>	<u>10 ± 0.5</u>
Linear Gradient from T_{liq} at bottom to T_{wall}^{Top} at top	550	400	510	<u>10.6</u>	<u>11 ± 0.5</u>

This table summarizes the model predictions for the Li gas temperature, T_{gas} , which is readily translated into the predictions for the Li impinging rate onto the substrate and the accumulated Li thickness on the substrate.

Line 1) The model predicts the equilibrium condition, $T_{liq}=T_{gas}$ when no atoms can escape and all surfaces are at T_{liq} . The predicted thickness, about 3-times the measured value, is the thickness that would deposit on an area the size of the aperture *but, with this surface at T_{liq} , nothing would actually condense.*

Line 2) With the substrate at the proper temperature and atoms escaping through the gap the predicted thickness is about 50 % too high.

Line 3) With the substrate at the proper temperature and NO atoms escaping through the gap the predicted thickness is about 70 % too high.

Lines 4 & 5) With isothermal walls, at the temperature extremes of T_{wall}^{Top} , the predicted thickness is about half the measured thickness.

Lines 6 & 7) **The full linear gradient model. With all sources, sinks and temperature gradients included, the model predicts, within instrumental error, the correct Li thickness for the two measured extremes of T_{wall}^{Top} .**

The fact that this wall dominated model predicts the thickness so well also lends credence to the sticking coefficient model, embodied in Equation 2, and its assumptions relating to the independence of the thermally driven absorption and emission processes. These assumptions are: all species that hit a surface stick initially; the impingement rate is calculated from $W(T_{\text{gas}})$; *independent* of impingement, some species are emitted from the surface; the emission rate from the condensed material covering any surface is calculated from $W(T_{\text{wall}})$; and it is only the temperature difference $T_{\text{gas}}-T_{\text{liq}}$ that governs the accumulation, or depletion, of species at a surface. Thus, this model can also be used to calculate sticking coefficients, from first principles, in any system when chemical reactions or physical bombardment processes are either not present or not significant.

Implicit in the above analysis was the assumption that the volume of Li gas bounded by the liquid surface, substrate and crucible walls is isothermal. We have seen that the walls are not isothermal. However, the walls have much larger thermal mass than the volume of Li gas and thermal communication across, and through, the walls is by conduction. Thermal communication across the Li gas volume is by diffusion and collisions between the gas atoms, and between the gas atoms and the walls. We will now argue that this process is much faster than the wall conductance processes in this instance. Using the standard Kinetic Theory of Gasses⁴, the partial pressure, rms atomic velocity and mean free path of the gaseous Li atoms can be estimated. These values allow some general conclusions to be drawn concerning energy transport within the Li gas as follows.

The Li gas pressure is estimated to be about 10^{-2} torr by equating $W(T_{\text{gas}})$ to the standard (pressure/temperature/molecular weight/molecular radius)-dependent impingement rate from Kinetic Theory⁴. T_{gas} is calculated from Equation 4.2. The Li atom mean free path is then found to be on the order of 2-3 cm while the average velocity of a Li atom is on the order of 2×10^5 cm/s. The longest distance within the crucible is about 25 cm. This 25 cm straight line distance is roughly 10 times as long as the mean free path between collisions. Thus, with collisions, to random walk the 25 cm will take about 100 steps/collisions and will require about 1 millisecond to complete. Therefore, carrying the kinetic calculations further, there are about 8×10^{14} Li atoms in every cubic centimeter communicating intimately 1000 times per second with only $\sim 3 \times 10^3$ other cubic centimeters within the volume. It is therefore reasonable to assume that the gas can respond to temperature fluctuations in the surroundings, and regain an isothermal profile within a small fraction of a second after a fluctuation since,

typically, after only 10 collisions thermalization is generally assumed to be complete. Thus, even though the walls support a large temperature gradient, the high speed of thermalization within the gas (relative to within the walls) should permit the gas volume to maintain relatively isothermal conditions. It is even more reasonable to assume that, in light of the very slow thermal response of the crucible, the isothermal Li gas assumption would be valid when averaging over the 21 second exposure time of the web moving past the aperture at the top of the crucible during our standard deposition run. Now we turn to a discussion about the heat load delivered to the substrate.

MODELING THE HEAT LOAD TO THE SUBSTRATE: The web substrate can absorb energy from radiation incident upon the web from the surroundings and from the enthalpy of condensation of the Li atoms deposited onto the web. Energy may also leave the substrate as radiation as well as by conductive and/or convective transfer into the chill drum. The formulas for the radiative transfer of energy are easily found in the literature^{5,6} and they depend on the temperatures and emissivities of the surfaces involved as well as the relative field of view that the surfaces have of each other. The enthalpy of condensation contribution can be calculated directly from Equations 1 through 5 above and the Latent Heat of Vaporization (LHV) of Li ($LHV_{Li}=2.13 \times 10^4$ J/g). To use the heat equation to calculate the heat flow into the chill drum it is necessary to know the thermal conductivity of the web⁷ (Th_w) and the heat transfer coefficient (K_{hx}) between the drum and the web⁸. For PET¹, $Th_w=0.0017$ w/cm K. However K_{hx} depends on a number of factors and is highly process dependent as well as dependent upon the exact history of the PET. This is due to the fact that direct conduction proceeds only through a small fraction of the substrate area because the microscopically rough surfaces of the web and drum have very little actual contact area. A large contribution to K_{hx} is due to convection through vapors outgassed from the PET⁸. This outgassing rate is very sensitive to web temperature and to the amount of water and atmospheric gasses incorporated within the PET at the time the film was produced.

The mathematical details of our model for calculating the temperature rise of the substrate will appear at a later date. At this time we present only the *results of the calculation* for modeling our standard run, as defined above, with the following assumptions. We have taken the emissivity of the growing Li film to be 0.15 and have used the value of 0.01 w/cm² K for K_{hx} . The chosen emissivity of 0.15 is typical of metals with conductivity similar to Li metal and the heat transfer coefficient, $K_{hx}=0.01$ w/cm² K, was a very typical *measured* value from

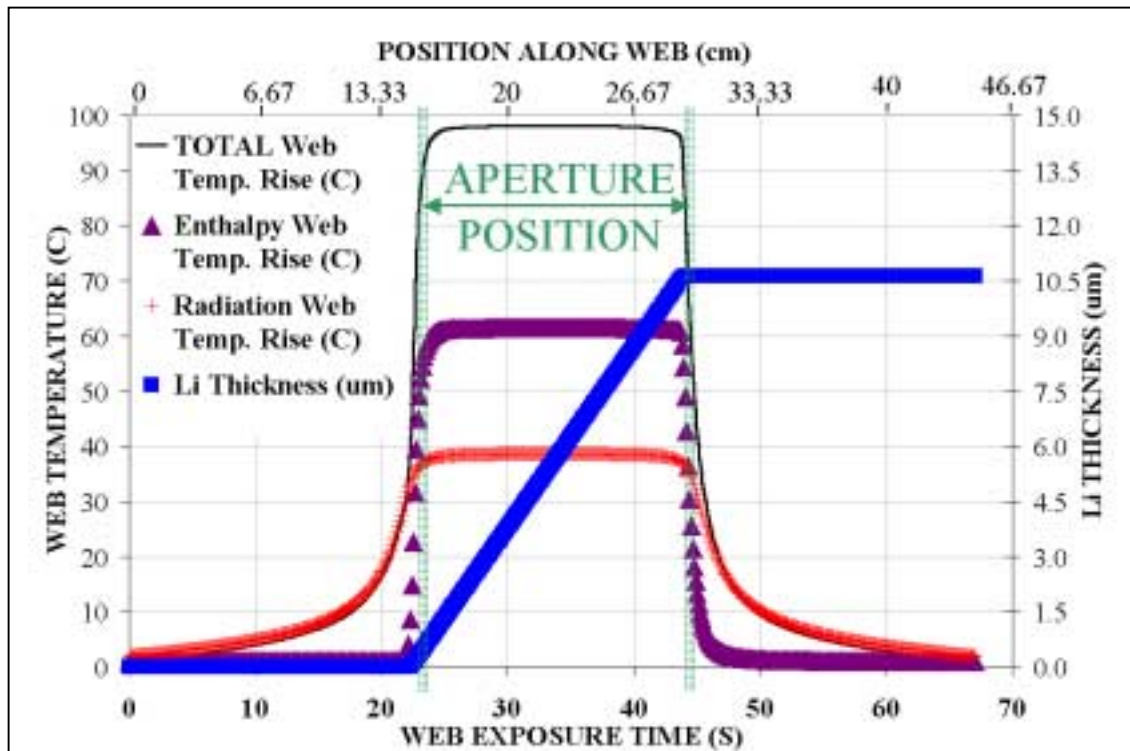


Figure 3. Results from our mathematical model for substrate heating. The substrate temperature profiles (total and individual contributions due to radiation and enthalpy of condensation), along with accumulated Li film thickness, as a function of position relative to the enclosure are shown. No variation of parameters was performed although emissivity was typical of metals with conductivity similar to Li metal and a reasonable literature value for the thermal conductivity of PET was used⁸. In these plots, the leading and trailing edges of the 14 cm long Li enclosure aperture are located at time indexes 22.5 s and 43.5 s, respectively. Thus, one sees the radiation heat flux becoming appreciable well before the web nears the box, and not vanishing until well after the web has left the area of the enclosure. Contrawise, the diffusion of Li flux out through the gaps only leads to deposition, and heat load, within 1-2 s of either edge.

the literature⁸. Figure 3 shows the model predictions with only these 2 free parameters.

From Figure 3 it is seen that the maximum temperature that the PET web is estimated to reach is about 98 C. This value is in between PET's glass transition temperature of $T_g=70$ C, and the maximum temperature, 120 C, at which it can

possibly retain its mechanical integrity. This value seems reasonable to us for two reasons. First, one would expect substrate damage to start to occur at a temperature in the vicinity of, but greater than, T_g . Second, the reason that $T_{liq}=550$ C is our standard run temperature is that 550 C is the highest temperature that we are able to run the liquid at, confidently, without damaging the substrate - NOTE that, for $T_{liq}=560$ C the model predicts a maximum web temperature of 120 C. Thus, we know that the substrate temperature is very near the damage threshold, which should be above T_g (70 C) and below 120 C. We also know that occasionally, if the web is tracking well and there are no other factors distorting the substrate, we can operate with the liquid temperature very slightly above 550 C without problems. Thus we are fairly certain that, with the liquid below 550 C, the web is safely below 120 C. Based on this information, the model prediction is not in conflict with the observations and it appears to be very reasonable.

It is also interesting to note that slightly more than 37% of the total heat load delivered to the substrate is due to radiation while the remainder is due to the enthalpy of condensation of the Li atoms. Further, for most of the 21 seconds that the web is exposed to the Li flux, thermally, the web is in steady state. The substrate temperature change, due to Li flux levels, is a rise from ambient to the maximum within 1-2 s on either side the leading edge of the evaporator aperture followed by a similarly swift fall back to ambient after passing the trailing edge. The radiation contribution to the temperature rise, on the other hand, is noticeable for more than 20 s before, and after, encountering the enclosure.

Based upon the modeling program, new evaporators, that should be more efficient (higher rate and less heat) have been designed, fabricated and are awaiting installation.

CONCLUSIONS: The thermodynamic model for calculation of evaporated flux works extremely well for Li and, based upon the general nature of its derivation, the model should be applicable to all thermal sources. This model is extremely useful as a design tool for building thermal sources since it allows precise calculations of how all temperature gradients affect the deposition rate. Thus, measurements of the temperature gradients in the operating system can be used as feedback for process control to allow accurate deposition thickness control even when the system is still moving through quasi-steady states toward its final steady state operating conditions. The utility of the model stems from its ability to calculate, a priori, the sticking coefficients from known thermodynamic

data³ from the literature that, in turn, permits calculation of the deposition rate. As an aside, the model should also prove useful in modeling distillation and assorted reflux processes.

Because this flux model is so accurate, it is an excellent starting point for the larger model that calculates the complete thermal flux to, and temperature rise of, the substrate during the deposition process. Once the source geometry is modeled so that the flux is accurately calculated, you automatically have the shape and temperature profile of the relevant radiation source as well. Thus, this thermodynamic model produces all of the data necessary to calculate the total thermal input to the substrate. It then remains only to develop the model for the mechanisms that cool the substrate, or govern the total thermal output. The results shown in Figure 3 indicate that our model for calculating the heat load to the substrate appears to work fairly well too. The model has shown us how to design more efficient sources that should be capable of higher rate with lower substrate heat loads.

Future work will involve in situ substrate temperature measurements and modeling the exact nature of the heat transfer coefficient between the substrate and the chill drum.

REFERENCES:

¹ DuPont Mylar product literature at <http://www.dupont.com/packaging/products/films>.

² Physical properties for Li at <http://www.webelements.com/>.

³ S. Dushman, "Scientific Foundations of Vacuum Technique", edited by J.M. Lafferty, John Wiley and Sons, chapter 10, pg. 695-737, 1962.

⁴ S. Dushman, "Scientific Foundations of Vacuum Technique", edited by J.M. Lafferty, John Wiley and Sons, chapter 1, pg. 1-79, 1962.

⁵ Bennett and Myers, "Momentum, Heat and Mass Transfer", McGraw Hill, 3rd ed., p442, 1982.

⁶ Schaums Outlines, "Heat Transfer" 2nd ed., p306.

⁷ J.P. Holman, "Heat Transfer", McGraw Hill, pg. 2, 1962.

⁸ M. Roehrig, C. Bright and D. Evans, "Vacuum Heat Transfer Models for Web Substrates: Review of Theory and Experimental Heat Transfer Data", 43rd Annual Tech. Proc. of the SVC, pg. 335-341, 2000.